AMP-activated protein kinase: greater AMP dependence, and preferential nuclear localization, of complexes containing the α2 isoform

Ian SALT*, Jakub W. CELLER*, Simon A. HAWLEY*, Alan PRESCOTT*, Angela WOODS†, David CARLING† and D. Grahame HARDIE*[1]

*Biochemistry Department, The University, Dundee DD1 4HN, Scotland, U.K., and †MRC Molecular Medicine Group, Imperial College School of Medicine, Hammersmith Hospital, Du Cane Road, London W12 0NN, U.K.

Mammalian AMP-activated protein kinase (AMPK) is the downstream component of a cascade that is activated by cellular stresses associated with ATP depletion. AMPK exists as heterotrimeric αβγ complexes, where the catalytic subunit has two isoforms (α1 and α2) with different tissue distributions. The budding yeast homologue is the SNF1 kinase complex, which is essential for derepression of glucose-repressed genes, and seems to act by the direct phosphorylation of transcription factors in the nucleus. AMPK complexes containing the α2 rather than the α1 isoform have a greater dependence on AMP (approx. 5-fold stimulation compared with approx. 2-fold) both in direct allosteric activation and in reactivation by the upstream kinase. We have also examined their subcellular localization by using Western blotting of nuclear preparations, and by using two detection methods in the confocal microscope, i.e. indirect immunofluorescence of endogenous proteins and transfection of DNA species encoding green fluorescent protein–α-subunit fusions. By all three methods a significant proportion of α2, but not α1, is localized in the nucleus. Like SNF1, AMPK-α2 complexes could therefore be involved in the direct regulation of gene expression. The observed differences in the regulation of α1 and α2 complexes by AMP might result in differential responses to ATP depletion in distinct cellular and subcellular locations.

INTRODUCTION

The AMP-activated protein kinase (AMPK) is the downstream component of a protein kinase cascade that is activated by cellular stresses resulting in ATP depletion, thus acting like a 'fuel gauge' [1]. The cascade is activated by stresses such as heat shock [2], prolonged exercise [3] or electrical stimulation [4] in skeletal muscle, and ischaemia in heart muscle [5], as well as inhibitors of the tricarboxylic acid cycle or oxidative phosphorylation such as arsenite [2], antimycin A, dinitrophenol and azide [6]. These treatments activate the cascade by lowering the ATP-to-ADP ratio, leading to an elevation in AMP via displacement of the adenylate kinase reaction ($2ADP \leftrightarrow ATP + AMP$). The increase in AMP, coupled with the decrease in ATP, activates the system via a multistep process involving the binding of AMP to both the upstream kinase, AMPK kinase (AMPKK), and to the downstream kinase, AMPK [7,8]. Activated AMPK then inhibits ATP-consuming anabolic pathways such as the synthesis of fatty acids and sterols [2,9] and activates ATP-generating catabolic pathways such as fatty acid oxidation [10].

Mammalian AMPK comprises three subunits [11], now termed α, β and γ [12,13], in a heterotrimeric complex. The α subunit contains the kinase domain at the N-terminus [14]. The functions of the non-catalytic β and γ subunits remain unclear, although all three subunits are required for the formation of a stable, fully active complex [13,15,16]. Both the α and the β subunits have recently been found to exist as two distinct gene products termed α1 and α2 [16,17], and β1 and β2 [18,19]. It has been unclear whether these isoforms have distinct functions. The α1 and β1 subunits seem to be rather widely expressed, whereas the α2 subunits are particularly highly expressed in skeletal and cardiac muscle and in liver [17], and the β2 subunit in skeletal muscle [19]. Vavvas et al. [20] recently reported that the activation of AMPK by the electrical stimulation of rat hindlimb muscle was restricted to the α2 isoform.

The α, β and γ subunits of AMPK all have clear homologues in the yeast *Saccharomyces cerevisiae*, i.e. the products of the *SNF1*, *SIP1/SIP2/GAL83* and *SNF4* genes respectively. Snf1p and Snf4p form a complex [21–23], whereas Sip1p, Sip2p and Gal83p are also associated with the complex and seem to represent alternative β subunits [24,25]. The yeast SNF1 complex and mammalian AMPK share at least one common physiological substrate, namely acetyl-CoA carboxylase, the key regulatory enzyme of fatty acid synthesis [26–28]. However, genetic evidence suggests that the major role of SNF1 is in regulating gene expression and, consistent with their roles in regulating gene expression as well as metabolism, both Snf1p and Snf4p are found in the nucleus as well as in the cytoplasm [21,29]. The *SNF1* and *SNF4* genes were originally defined as mutations that would not grow on sucrose, and both are required for the derepression of genes that are repressed in the presence of glucose [30,31].

In this paper we address the question of whether there are functional differences between AMPK complexes containing the α1 and α2 isoforms of the catalytic subunit, particularly with respect to (1) regulation by AMP and (2) subcellular localization. We were particularly interested in whether either isoform might be localized in the nucleus, given the role of the yeast homologue

Abbreviations used: AMPK, AMP-activated protein kinase; AMPKK, AMPK kinase; CaMKK, calmodulin-dependent protein kinase I kinase; GFP, green fluorescent protein; PP2A, protein phosphatase 2A; PP2C, protein phosphatase 2C.

[1] To whom correspondence should be addressed (e-mail d.g.hardie@dundee.ac.uk).

in the regulation of gene expression. We report that complexes containing the $\alpha 2$ subunit are more dependent on AMP than are those containing the $\alpha 1$ subunit, with respect both to direct allosteric activation and to activation by the upstream kinase. By using three different approaches we also find that a large proportion of the $\alpha 2$ isoform is localized in the nucleus.

EXPERIMENTAL

Proteins and peptides

AMPK was purified from rat liver as far as the gel-filtration step [32]. In specific cases mentioned in the text, purification was only as far as step 1 [poly(ethylene glycol) precipitation] or step 2 (DEAE-Sepharose). AMPKK was purified from rat liver as far as the Mono Q step [32] and did not contain detectable AMPK activity. The catalytic subunit of protein phosphatase 2A (PP2A) was prepared from bovine heart with a procedure described for rabbit muscle [33]. Protein phosphatase 2C (PP2C; human α-isoform) was purified after expression in *Escherichia coli* [7]. Calmodulin-dependent protein kinase I kinase (CaMKK) (an equimolar mixture of α and β isoforms) was purified from rat brain [34]. Agarose-bound 5′-nucleotidase from *Crotalus adamanteus* venom was from Sigma.

The 'SAMS' peptide (HMRSAMSGLHLVKRR) [35], and the 'AMARA' (AMARAASAAALARRR) peptide and its variant (AMARAASAAAGARRR) [36], were synthesized as described previously.

Immunological reagents

Protein G–Sepharose was from Pharmacia Biotech. Horseradish peroxidase-linked rabbit anti-(sheep IgG) was from Pierce and Warriner. Texas Red-linked donkey anti-(sheep IgG) was from Jackson Laboratories. Murine monoclonal anti-(green fluorescent protein) (anti-GFP) antibody was from Boehringer. Horseradish peroxidase-linked sheep anti-(mouse IgG) was from the Scottish Antibody Production Unit, Carluke, Scotland, U.K. Murine monoclonal anti-coilin antibody was a gift from Angus Lamond. Sheep antibodies against the AMPK-$\alpha 1$ and AMPK-$\alpha 2$ subunits were produced as described previously [16]. Sheep antibodies against the AMPK-β subunits were raised against the C-terminal peptide LSATHRYKKKYVTT as described for the α subunit antibodies [16].

Plasmids

cDNA species encoding the AMPK $\alpha 1$, $\alpha 2$, $\beta 1$ and $\gamma 1$ subunits were in the mammalian expression vector pcDNA3 [16]. The GFP fusions were constructed by using the plasmid phGFPmcs, which was made by inserting a multiple cloning site between the *Bsr*GI and *Not*I sites of phGFP-S65T (Clontech). A *Hin*dIII fragment of phGFPmcs was cloned into pcDNA3, and *Eco*RI/*Xho*I and *Eco*RI fragments encoding $\alpha 1$ and $\alpha 2$ respectively were inserted into the corresponding restriction sites within the polylinker of the resulting plasmids. These constructs have GFP fused in-frame at the N-termini of $\alpha 1$ and $\alpha 2$.

Enzyme assays

AMPK was assayed as described previously [35], except that where stated the 'AMARA' peptide (200 μM) was used as substrate in place of 'SAMS' [32]. Results were corrected for radioactivity recovered in blank reactions lacking peptide. Protein phosphatases were assayed as described [33,37]. One unit of AMPK and protein phosphatases is defined as the quantity transferring/removing 1 nmol of phosphate/min at 30 °C. AMPKK was assayed as described previously [32].

Immunoprecipitation of AMPK isoforms and GFP–α subunit fusions

Sheep anti-AMPK antibodies were prebound to 80 μl of 25 % (w/v) Protein G–Sepharose in IP buffer [50 mM Tris/HCl (pH 7.4 at 4 °C)/150 mM NaCl/50 mM NaF/1 mM sodium pyrophosphate/1 mM EDTA/1 mM EGTA/1 mM dithiothreitol/0.1 mM benzamidine/0.1 mM PMSF/5 μg/ml soybean trypsin inhibitor/1 % (v/v) Triton X-100] by incubation for 1 h at 4 °C on a roller mixer. The mixture was then centrifuged (14000 ***g***; 30 s; 4 °C) and the pellet was washed five times with 1 ml of IP buffer. AMPK was diluted in IP buffer, added to the Protein G–Sepharose pellet and incubated on the roller mixer for 2 h at 4 °C. The mixture was then centrifuged (14000 ***g***; 30 s; 4 °C) and the immunodepleted supernatant was used for further experiments. In experiments in which the immunoprecipitate was assayed for AMPK activity, it was first washed five times with 1 ml of IP buffer containing 1 M NaCl (to remove non-specifically bound proteins) before resuspension in assay buffer.

Immunoprecipitation with anti-GFP antibody was performed in the same way, except that sheep anti-(mouse IgG) was prebound to the Protein G–Sepharose (by the method above) before the binding of the mouse anti-GFP antibody.

Dephosphorylation of AMPK isoforms

AMPK isoforms were prepared by immunodepletion as described above except that the NaF and pyrophosphate were replaced by 50 mM NaCl. For dephosphorylation with PP2C, EDTA and EGTA were also replaced by 5 mM $MgCl_2$. AMPK was incubated at 30 °C with PP2A or PP2C and, at intervals, 5 μl aliquots were removed and assayed for AMPK activity with 200 nM okadaic acid (PP2A) or 50 mM NaF (PP2C) in the assay buffer.

Cell culture

INS-1 cells were grown in RPMI 1640 supplemented with 10 % (v/v) heat-inactivated fetal bovine serum, 10 mM Hepes, 2 mM glutamine, 1 mM pyruvate, 50 μM 2-mercaptoethanol, 100 i.u./ml penicillin and 100 μg/ml streptomycin. CCL13 cells were cultured in Dulbecco's modified Eagle's medium with 10 % (v/v) fetal calf serum. Both cell lines were maintained at 37 °C in air/CO_2 (19:1).

Subcellular fractionation of INS-1 cells

Cells were harvested by treatment with trypsin, washed twice in 30 vol. of ice-cold PBS [137 mM NaCl/3 mM KCl/100 mM phosphate (pH 7.4 at 4 °C)] and centrifuged (1200 ***g***; 5 min; 4 °C). Whole-cell lysates were prepared by the addition of 20 times the packed cell volume of ice-cold lysis buffer [50 mM Tris/HCl (pH 7.4 at 4 °C)/250 mM mannitol/50 mM NaF/1 mM sodium pyrophosphate/1 mM EDTA/1 mM EGTA/1 mM dithiothreitol/0.1 mM benzamidine/0.1 mM PMSF/5 μg/ml soybean trypsin inhibitor/1 % (v/v) Triton X-100]. Lysates were homogenized by 20 passes in a Dounce homogenizer, vortex-mixed and centrifuged (14000 ***g***; 3 min; 4 °C). The supernatant was decanted, snap-frozen and stored at −80 °C. Nuclear extracts were prepared by gently resuspending packed cells in an equal volume of hypotonic buffer [10 mM Hepes (pH 8.0)/10 mM KCl/1.5 mM $MgCl_2$/1 mM dithiothreitol] and allowing them to swell on ice for 15 min. The cells were lysed by passing them 20 times through a narrow gauge (25G) needle. The resultant

homogenate was centrifuged (14000 *g*; 30 s; 4 °C) to produce a nuclear pellet. The pellet was washed three times with 1 ml of hypotonic buffer and then resuspended in two-thirds of the packed cell volume of hypertonic buffer [20 mM Hepes (pH 8.0)/600 mM KCl/0.2 mM EDTA/1 mM dithiothreitol/0.5 mM PMSF/25 % (v/v) glycerol] and mixed for 30 min at 4 °C. Nuclear debris was pelleted by centrifugation (14000 *g*; 4 °C; 5 min). The supernatant was decanted, snap-frozen in liquid N_2 and stored at −80 °C.

Western blots

Samples were resolved by SDS/PAGE and transferred to a nitrocellulose membrane. The membranes were blocked by incubation in TBS-Tween [20 mM Tris/HCl (pH 7.4)/137 mM NaCl/0.05 % (v/v) Tween 20] supplemented with 3 % (w/v) low-fat milk powder for 1 h at room temperature. The primary antibody was applied in the same buffer and the blots were incubated for a further 2 h at room temperature. After extensive washing with TBS-Tween, the blots were incubated for 1 h at room temperature with either horseradish peroxidase-linked rabbit anti-(sheep IgG) (for sheep antibodies) or horseradish peroxidase-linked rabbit anti-(mouse IgG) (for mouse antibodies). After further extensive washing, the blots were developed by using enhanced chemiluminescence (Amersham).

Immunolabelling of fixed cells

Cells were seeded in six-well plates at a density of 4×10^5 INS-1 cells or 5×10^5 CCL13 cells per well, with two circular coverslips 10 mm in diameter in each well. The plates were grown in culture for 4–5 days before fixation. The media were removed and cells were preincubated in 2 ml per well of KRH buffer [20 mM Hepes (pH 7.4)/119 mM NaCl/5 mM $NaHCO_3$/4.75 mM KCl/1.3 mM $CaCl_2$/1.2 mM $MgSO_4$/0.1 % (w/v) BSA] supplemented with 10 mM glucose at 37 °C for 60 min. The preincubation buffer was removed and replaced with 2 ml of KRH buffer per well, with or without glucose or other test substance, and incubated for a further 60 min at 37 °C. The cells were then fixed by incubation in 4 ml of 4 % (w/v) paraformaldehyde in PBS at room temperature for 10 min. The cells were washed three times with 5 ml of PBS per well and permeabilized by incubation in PBS supplemented with 1 % (v/v) Nonidet P40 for 20 min. Coverslips were removed and 70 μl of donkey serum, diluted 1:10 with PBS, was added to block non-specific binding sites. Coverslips were washed thoroughly with PBS and incubated for 1 h with 70 μl of sheep anti-AMPK antibodies. The coverslips were again washed thoroughly with PBS and incubated for 1 h with Texas Red-linked donkey anti-sheep IgG. Coverslips were again thoroughly washed with PBS and then mounted on slides. A drop of Citifluor glycerol/PBS reagent was placed on each coverslip and a large coverslip was put on top. The slides were sealed with nail polish and stored at 4 °C until viewed on the confocal microscope.

Transfection of INS-1 and CCL13 cells

Cells were treated with trypsin, pelleted by centrifugation and resuspended in electroporation medium in 400 μl aliquots containing 4×10^6 cells. Plasmids encoding AMPK subunits previously prepared with the EndoFree Plasmid Maxi Kit (Qiagen) were added (5 μg of DNA for each subunit/electroporation aliquot). The aliquots were placed in the electroporation cuvettes (Invitrogen) with an electrode gap of 4 mm. Electroporation was performed with an Easyject plus apparatus (Equibio) set for a single pulse at 240 V, 900 μF and infinite resistance. Immediately after electroporation the cells were transferred to cell culture dishes 100 mm in diameter containing 10 ml of culture medium, and grown in culture for 20 h.

Confocal microscopy

Cells were imaged on a Bio-Rad MRC 600 laser scanning confocal microscope mounted on a Nikon Microphot-SA microscope. During imaging all settings were kept constant, i.e. laser power, photomultiplier tube amplification and pinhole size were maintained. Fixed cells were imaged with a Nikon ×60 Plan Apo (NA 1.4) oil-immersion objective and living cells were imaged with a Zeiss X40 plan-Neofluor (NA 0.9) multi-immersion objective. Digitally recorded images were exported to Adobe Photoshop and printed on a Kodak DS 8650 PS dye-sublimation printer. Mean pixel fluorescence intensities in the nucleus and cytoplasm were estimated with Bio-Rad COMOS software.

RESULTS

AMP-dependence of α1 and α2 complexes purified from rat liver

The starting material used for separation of the α1 and α2 isoforms was AMPK purified 500-fold from rat liver [32], which in terms of kinase activity is an approx. 1:2 mixture of the α1 and α2 isoforms [16]. The preparation from which the samples in Figure 1 were derived was stimulated 2.5-fold by 200 μM AMP, and this was not affected by a mock immunoprecipitation with control antibody. Saturating amounts of α2 or α1 antibody precipitated approx. 65 % and approx. 35 % of the activity respectively as expected: the kinase remaining in solution was found by Western blotting (results not shown) to be exclusively α1 and α2 respectively, and was used for further experiments. Figure 1 shows that both isoforms were activated by similar concentrations of AMP, but that the degree of stimulation of the α2 form was much greater than that of the α1 form. The α2 form was stimulated 5.5 ± 0.3-fold by AMP (mean ± S.E.M.; see Figure 1 legend) with a half-maximal effect at 22 ± 3 μM. The α1 form

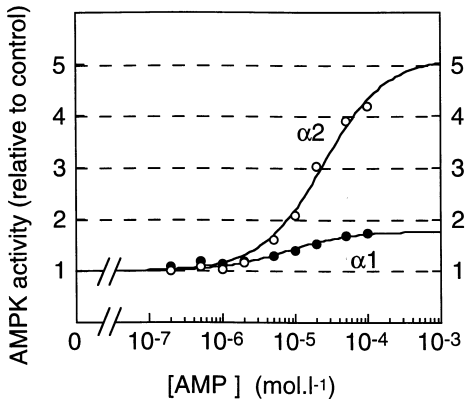

Figure 1 AMP dependence of isolated α1 (●) and α2 (○) forms of AMPK

Isoform-specific complexes were prepared by immunodepletion of the other form from purified rat liver enzyme, then assayed at different concentrations of AMP. Data were fitted to the equation $v = b + \{[(s \times b) - b] \times [AMP]\}/(A_{0.5} + [AMP])$, where b is basal activity, s is relative stimulation and $A_{0.5}$ is the concentration of AMP giving half-maximal activation, by using Kaleidagraph (Abelbeck software). Values for stimulation by AMP and $A_{0.5}$ are presented in the text as means ± S.E.M. Circles represent the data points; the theoretical curves were generated by the curve-fitting procedure. The results are expressed relative to the basal activity in the absence of AMP: the basal activities in the immunodepleted supernatants were 0.54 (α1) and 0.45 (α2) nmol/min per mg.

Table 1 Degree of AMP stimulation of AMPK prepared by immunoprecipitation after the first two steps of purification, i.e. poly(ethylene glycol) (PEG) precipitation and DEAE-Sepharose chromatography

The PEG precipitates were prepared by dissecting out the rat livers at ambient temperature, or by freeze-clamping. The DEAE-Sepharose fraction was prepared by dissecting out the rat livers at ambient temperature. Recovery refers to the percentage of the original total AMPK activity in the fraction recovered in the immunoprecipitate. Total recovery in the $\alpha1$ plus the $\alpha2$ (or anti-γ) immunoprecipitates was 90–100% in each case. Absolute activities were 2–4-fold higher (mean ± S.E.M. 2.7 ± 0.3-fold) in the precipitates prepared by dissection at ambient temperature rather than by freeze-clamping.

	Anti-$\alpha1$		Anti-$\alpha2$		Anti-γ
	Recovery (%)	Stimulation (fold)	Recovery (%)	Stimulation (fold)	Stimulation (fold)
PEG precipitate (ambient)	36	2.0	56	6.6	4.6
PEG precipitate (freeze-clamped)	38	1.4	62	5.3	4.0
DEAE-Sepharose	40	2.7	57	6.3	4.3
Mean ± S.D.	38 ± 2	2.0 ± 0.7	58 ± 3	6.1 ± 0.7	4.3 ± 0.3

was stimulated only 1.7 ± 0.1-fold by AMP, with a half-maximal effect at 12 ± 3 μM. Similar results were obtained when the $\alpha1$ and $\alpha2$ isoforms were separated from at least three independent preparations of AMPK. The activity in the absence of added AMP was unaffected by addition of snake venom 5′-nucleotidase, showing that no endogenous AMP was present.

The lower AMP-dependence of the $\alpha1$ complexes might have been an artifact caused by selective loss of AMP-dependence during the six steps of purification before immunodepletion. It is normally difficult to measure AMP stimulation during the early stages of AMPK purification owing to contamination of fractions by AMP and/or adenylate kinase (which can generate AMP from ADP formed in the kinase reaction). We therefore examined the effects of AMP in well-washed immunoprecipitates prepared after step 1 [poly(ethylene glycol) precipitation] or step 2 (DEAE-Sepharose) of the purification. Step 1 enzyme was made both after harvesting the liver at ambient temperature and after harvesting it by freeze clamping. The kinase activities are higher in the former case because the enzyme is activated by phosphorylation caused by increases in AMP concentration *post mortem* that occur while the tissue is being harvested [26]. Immunoprecipitates were made with anti-$\alpha1$ and anti-$\alpha2$ antibodies, and also with an anti-γ antibody, which precipitates both forms. The results (Table 1) show that the lower degree of stimulation of the $\alpha1$ complexes was also observed after the earlier steps, suggesting that it was not an artifact of purification. The mean stimulation of the $\alpha1$ complexes (38 ± 2% of the activity recovered in the anti-γ precipitate, measured in the presence of AMP) in the three different samples was 2.0 ± 0.7-fold, and for the $\alpha2$ complex (58 ± 3% of the activity in the anti-γ precipitate) was 6.1 ± 0.7-fold. The stimulation of the complexes precipitated by anti-γ antibody was 4.3 ± 0.3-fold, which as expected was intermediate between that of the $\alpha1$ and $\alpha2$ complexes. The results in the poly(ethylene glycol) precipitates were not significantly affected by whether the livers were sampled by dissection at ambient temperature or by freeze-clamping, although as expected the absolute kinase activities were higher (by 2.7 ± 0.3-fold, mean ± S.E.M. for six observations) in the former case.

Dephosphorylation and rephosphorylation of the $\alpha1$ and $\alpha2$ isoforms from rat liver

The threonine residue (Thr-172) that we have identified as being the primary site for phosphorylation by the upstream kinase, AMPKK [32], and the sequence immediately surrounding it, are highly conserved between the $\alpha1$ and $\alpha2$ isoforms. If $\alpha1$ or $\alpha2$ were prepared by immunodepletion of the other isoform, both activities were stable during incubation at 30 °C in the absence of added phosphatases (results not shown). When PP2C (human α isoform) was added in the presence of Mg^{2+}, both $\alpha1$ and $\alpha2$ were inactivated (Figure 2). The $\alpha2$ isoform was also readily inactivated with PP2A (bovine heart catalytic subunit) but the $\alpha1$ form was more resistant to inactivation by this phosphatase. After dephosphorylation with either PP2C or PP2A, both isoforms could be reactivated by addition of the upstream kinase, AMPKK, in

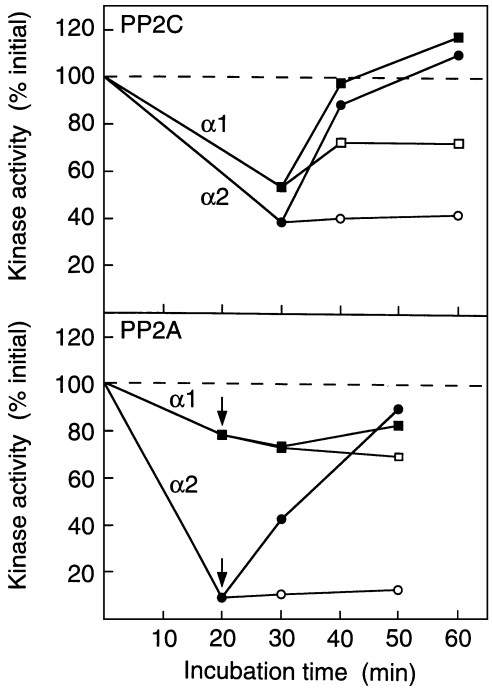

Figure 2 Inactivation of the $\alpha1$ (□,■) and $\alpha2$ (○,●) forms of AMPK by PP2C (upper panel) and PP2A (lower panel), and subsequent reactivation by AMPKK plus MgATP^{2-}

Isoform-specific complexes prepared as for Figure 1 were inactivated by treating with PP2C (8 units/ml) or PP2A (8 units/ml) for 20 min. At the point shown by the arrow, okadaic acid (100 nM) was added to inhibit further dephosphorylation, together with 5 mM $MgCl_2$, 200 μM ATP and 100 μM AMP, either with (■, ●) or without (□, ○) AMPKK (5000 units/ml). At various times, aliquots were removed for AMPK assay with the 'AMARA' peptide as substrate [32].

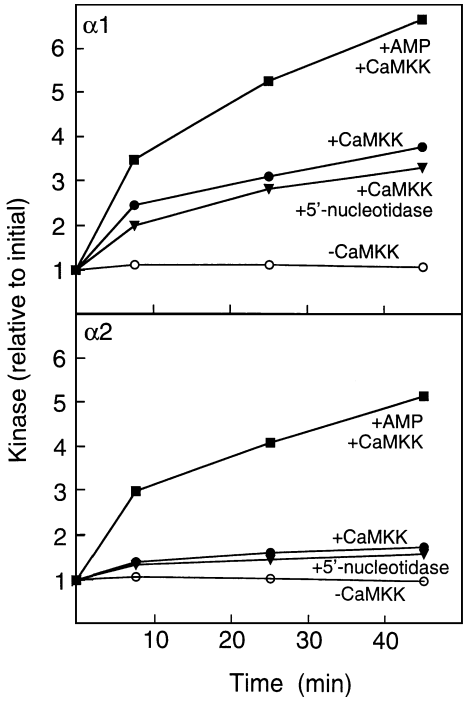

Figure 3 Effect of 5′-AMP on reactivation of α1 and α2 complexes by CaMKK

AMPK complexes containing the α1 isoform (top panel) or α2 isoform (bottom panel) were inactivated by treatment with high concentrations of PP2A (125 units/ml) for 15 min. Okadaic acid (500 nM) was added and incubation was continued with the following additions: $MgCl_2$ (5 mM) and ATP (200 μM) alone (○), CaMKK (0.28 μg/ml) plus $MgCl_2$/ATP (●), CaMKK plus $MgCl_2$/ATP plus 100 μM AMP (■) or CaMKK plus $MgCl_2$/ATP plus 60 m-units/ml 5′-nucleotidase (▼). At various times aliquots were removed for AMPK assay with the 'AMARA' peptide as substrate [32].

the presence of $MgATP^{2-}$: little or no reactivation occurred on addition of $MgATP^{2-}$ alone.

Effects of AMP on reactivation of the α1 and α2 isoforms from rat liver

As well as causing direct allosteric activation, the binding of 5′-AMP to AMPK also makes it a better substrate for the upstream kinase, AMPKK, and for another kinase that can mimic the effect of AMPKK *in vitro*, namely CaMKK [8]. To examine whether α1 or α2 complexes differed in their requirements for AMP for phosphorylation and reactivation, we utilized CaMKK as the upstream kinase. This has the advantage that, unlike AMPKK, AMP has no effect on CaMKK, so that any effects of the nucleotide would be entirely substrate mediated. Figure 3 shows that the reactivation of the rat liver α1 complex by CaMKK was stimulated approx. 2-fold by AMP, whereas reactivation of the α2 complex was stimulated 5-fold. The greater AMP dependence of the α2 complex was therefore observed in the phosphorylation reaction as well as in direct allosteric activation. The reactivation of either complex in the absence of AMP was not significantly affected by the addition of snake venom 5′-nucleotidase (Figure 3). This shows that the AMP-independent reactivation was not due to AMP that either contaminated the reagents or was generated from ATP during the course of the reaction.

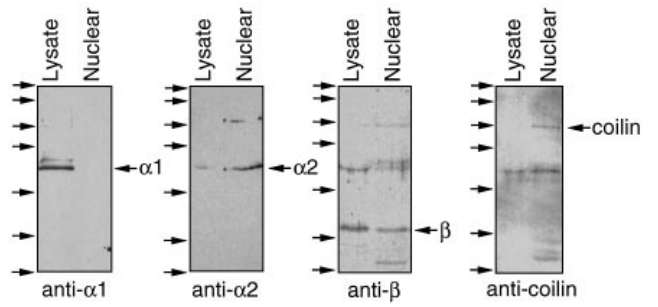

Figure 4 Western blotting of total cell lysates, and nuclear fractions, derived from INS1 cells

Blots were probed with antibodies against the α1, α2 and β subunits of AMPK, or with an antibody against a nuclear marker protein, coilin. Equal amounts of protein were loaded in the lysate and nucleus lanes. The arrows at the left of each blot show the migration of ProSieve protein markers [FMC BioProducts (Rockland, ME, U.S.A.); molecular masses in kDa from top to bottom: 225, 150, 100, 75, 50, 35, 25].

Substrate specificity of the α1 and α2 isoforms

In a previous paper [16] we reported small differences in specificity of the α1 and α2 isoforms purified from rat liver, especially with respect to the requirement for a hydrophobic side chain at the P+4 position (i.e. at four residues C-terminal to the phosphorylated serine). At a fixed peptide concentration of 40 μM, α2 complexes seemed to phosphorylate the peptide AMARAASAAAGARRR (which lacks a hydrophobic side chain at P+4) at a significant rate, whereas α1 complexes did not. To examine this in more detail, we determined kinetic parameters for this peptide by using both isoforms. The K_m values for α1 and α2 for this peptide were 920 ± 60 and 1560 ± 130 μM respectively. This compares with K_m values of 6.3 ± 0.8 μM (α1) and 13.1 ± 1.4 μM (α2) with the parent peptide (AMARAASAAALARRR), which does have a hydrophobic side chain (leucine) at P+4. Replacing the leucine residue at P+4 with glycine therefore causes a more than 100-fold increase in the K_m for both α1 and α2 complexes.

Nuclear localization of the α2 subunits determined by subcellular fractionation

We also examined whether there were differences in the subcellular localization of complexes containing the α1 and α2 isoforms. Because of the known role of the yeast homologue of AMPK (SNF1) in regulating gene expression, we were particularly interested in the question of whether either of the mammalian complexes might be localized in the nucleus. Nuclear fractions were prepared from INS-1 cells, a transformed cell line derived from rat pancreatic β-cells. Immunodepletion experiments similar to those used in the rat liver extracts showed that in extracts of these cells, α1 complexes accounted for approx. 90% of total AMPK activity, and α2 complexes for approx. 10%. The cells were washed to remove proteins in the medium and lysed by passage through a narrow-gauge needle in hypotonic medium. Nuclei were then prepared by differential centrifugation and extensive washing, and disrupted by extraction in hypertonic medium. Western blots were performed on equal protein loadings of the total cell lysate and the nuclear fractions (Figure 4). If anything, proteins in the total lysate are under-represented, because this fraction contained some serum albumin from the medium despite extensive washing of the cells. Probing of the blots with a monoclonal antibody against a nuclear marker (coilin) showed that it was highly enriched in the nuclear fraction.

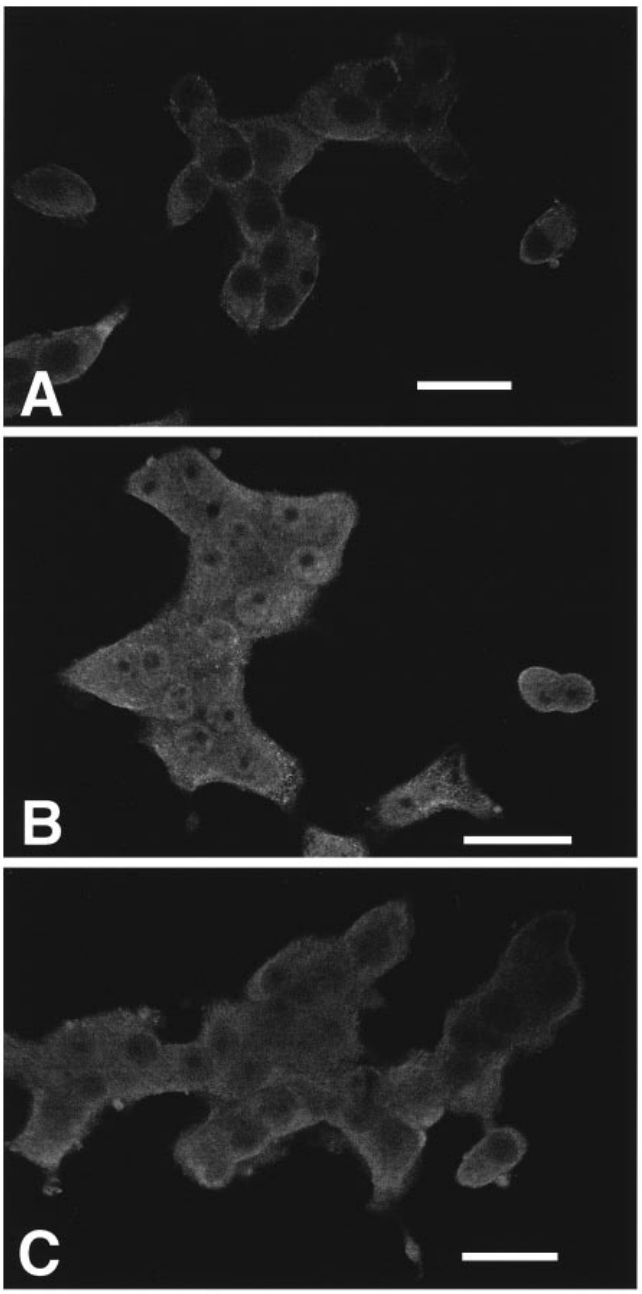

Figure 5 Confocal microscope images of INS-1 cells after indirect immunofluorescence detection with antibodies against the α1 (A), α2 (B) and β (C) subunits of AMPK

The very faint fluorescence in the nuclei of cells probed with α1 antibodies was similar to that seen when cells were probed with control antibody. Scale bars, 25 μm.

In the lysate fraction the α1 antibody detected the 63 kDa α1 polypeptide and one other polypeptide just above it that might represent phosphorylated α1. Neither was present in the nuclear fraction. The α2 antibody detected the 63 kDa α2 polypeptide and, faintly, an additional unknown polypeptide of approx. 100 kDa. Both were highly enriched in the nuclear fraction.

We also analysed the blots by using an anti-(β subunit) antibody. Although raised against a C-terminal sequence derived from the β1 isoform, this sequence is perfectly conserved in the β2 isoform [19], and the antibody recognizes both β1 and β2 after expression in CCL13 cells (results not shown). The cDNA species encoding β1 and β2 predict proteins of very similar molecular masses of approx. 30 kDa, but for unknown reasons both migrate anomalously on SDS/PAGE, β1 at an apparent molecular mass of 38 kDa and β2 at 34 kDa [19]. In INS-1 cell lysates the β subunit antibody recognized a polypeptide at 38 kDa (Figure 4), which co-migrated with the liver β1 subunit (results not shown). This suggests that β1, but not β2, is the predominant β subunit isoform in INS-1 cells. The β1 subunit was present in the nuclear fraction from INS-1 cells, although it did not seem to be as highly enriched in that fraction as α2 or coilin (Figure 4). The anti-β and coilin antibodies also non-specifically detect serum albumin when it is present in large amounts, and this accounts for the band migrating close to the α subunits in the anti-β and coilin blots.

Table 2 Cytoplasmic-to-nuclear ratio of mean pixel fluorescence intensity for INS-1 cells probed by indirect immunofluorescence with AMPK anti-subunit antibodies

Results are means $\pm$ S.E.M. for the numbers of cells shown in parentheses. Statistical analysis was by one-way analysis of variance, with Bonferroni's method. Statistical significances: **significantly different from equivalent value for α1 subunit ($P < 0.001$); †significantly different from equivalent value for α2 subunit ($P < 0.01$).

	Fluorescence intensity ratio, cytoplasm to nucleus	
Subunit	With glucose	Without glucose
α1	2.13 $\pm$ 0.05 (27)	2.13 $\pm$ 0.06 (24)
α2	1.09 $\pm$ 0.05 (19)**	1.13 $\pm$ 0.05 (18)**
β	1.35 $\pm$ 0.02 (21)**†	1.49 $\pm$ 0.06 (10)**†

Nuclear localization of AMPK subunits determined by indirect immunofluorescence in the confocal microscope

We next studied the localization of AMPK subunit isoforms by indirect immunofluorescence microscopy in INS-1 cells, and in the rat hepatoma cell line CCL13. Results for the INS-1 cells, which grow in small clumps resembling islets of Langerhans, are shown in Figure 5. Control experiments with preimmune serum and second antibody (results not shown) gave a faint background fluorescence that was distributed uniformly throughout the cells. Results with anti-α1 antibody (Figure 5A) suggested that α1 complexes were largely cytoplasmic, with the ratio of mean pixel fluorescence intensity (cytoplasm to nucleus) being more than 2:1 (Table 2). This is probably an underestimate of the true ratio because the fluorescence in the nuclei of cells labelled with α1 antibody was similar to the background with preimmune controls (results not shown). The anti-α1 fluorescence was distributed diffusely throughout the cytoplasm, although in some cells there did seem to be zones of brighter fluorescence at or near to the plasma membrane. In contrast with the results for α1, when the cells were probed with the anti-α2 antibody (Figure 5B) the fluorescence in the nucleus was well above the background level, being broadly distributed throughout this organelle although excluded from the nucleolus. Some α2 was also detectable in the cytoplasm, where it seemed to be associated with particulate structures near the plasma membrane. The ratio of cytoplasmic to nuclear fluorescence was approx. 1:1 (Table 2), which was significantly different from the results with α1 ($P < 0.001$). Qualitatively similar results were obtained with α1 and α2 antibodies in CCL13 cells (results not shown), although the

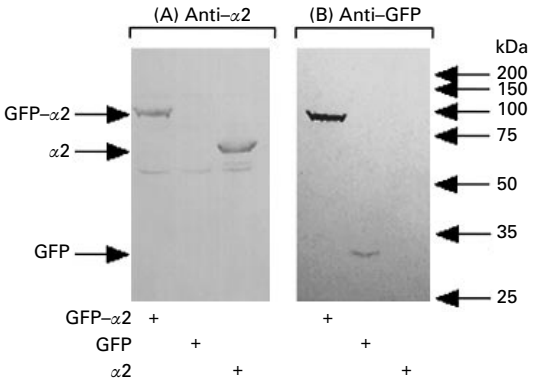

Figure 6 Western blotting of lysates of CCL13 cells transfected with DNA species encoding the GFP–α2 fusion, free GFP or free α2

DNA species encoding β1 and γ1 were co-transfected in each case. Blots were probed with anti-α2 antibody (**A**) or anti-GFP antibody (**B**).

background fluorescence with preimmune serum was somewhat higher in these cells. Starvation of the INS-1 cells for glucose, which activates AMPK (I. Salt, unpublished work), had no effect on the cytoplasmic-to-nuclear ratio for either α1 or α2 (Table 2).

When the antibody that recognizes both the β1 and β2 subunits was used, the distribution of β subunits was intermediate between that of α1 and α2, with stronger fluorescence in the cytoplasm, but a significant level in the nucleus (Figure 5C). In this case the ratio of cytoplasmic to nuclear fluorescence was approx. 1.4:1 (Table 2), which was significantly different from the ratios with either α1 ($P < 0.001$) or α2 ($P < 0.01$). This is the result expected on the assumption that the predominant β subunit in INS-1 cells (which seems to be β1; see above) associates with both α1 and α2.

Nuclear localization of AMPK subunits determined by expression of GFP fusions

To allow the study of the localization of the α subunits in living cells, we constructed expression plasmids encoding constructs in which GFP (S65T variant) from *Aequorea victoria* was fused at the N-terminus of the α1 or α2 subunits. Plasmids encoding free GFP, free α1 or α2 subunits, or GFP–α1/GFP–α2 fusions were transfected into CCL13 or INS-1 cells by electroporation, and expression of the products was studied by Western blotting, immunoprecipitation and confocal microscopy. Plasmids encoding AMPK-β1 (or AMPK-β2) and AMPK-γ1 subunits were co-transfected in every case. The 63 kDa α2 polypeptide was readily detectable (with anti-α2 antibodies) in blots of lysates from CCL13 cells transfected with plasmids encoding α2 but not in lysates of cells transfected with free GFP. If cells were transfected with DNA encoding a GFP–α2 fusion, a protein of the expected size (90 kDa) could be detected with either anti-α2 (Figure 6A) or anti-GFP (Figure 6B) antibody. With the anti-GFP antibody, a protein of 27 kDa could be detected in cells expressing free GFP, but there was no trace of polypeptides below 90 kDa in cells expressing GFP–α2. This shows that the GFP–α2 fusion is stable and is not degraded in the intact cells.

Very similar results were obtained with the α1 constructs (results not shown) except that endogenous α1 subunit (63 kDa) was detectable with anti-α1 antibody in cells expressing either GFP–α1 or free GFP. With the assumption that the antibodies bind with equal avidity to the free α1 subunit and to the GFP fusion (this is likely because the epitopes are not near the N-termini), densitometry showed that the expression of transfected GFP–α1 and free α1 subunits were similar and approx. 5-fold the level of the endogenous α1 subunit. Given that only 40–50 % of the CCL13 cells expressed the fluorescent fusion proteins, this indicates that the native α1 and the GFP–α1 fusion was over-expressed approx. 10-fold compared with the endogenous subunit. Owing to the much lower transfection efficiency in the INS-1 cells, we could not detect the GFP fusions by Western blotting of cell lysates. However, the fusion proteins were readily detected by fluorescence microscopy in the small proportion of cells that had been transfected (see Figure 7).

To confirm that the GFP fusions were active, we expressed α1, α2, GFP–α1, GFP–α2 or free GFP, together with β1 and γ1, in CCL13 and/or Chinese hamster ovary cells. We then immunoprecipitated with either anti-GFP, anti-α1 or anti-α2 antibodies and measured kinase activity in the precipitates. Table 3 shows results obtained with the α1 constructs in CCL13 cells. The cells contained a significant level of endogenous AMPK-α1 activity, as judged by the activity in the anti-α1 precipitate in cells expressing the free GFP plasmid. However, the activity in anti-α1 precipitates increased 2–3-fold in cells expressing recombinant α1 or GFP–α1, suggesting that the GFP fusion protein was approximately as active as the normal recombinant protein. The activity in the anti-α1 precipitates increased on expression of GFP–α1 by an amount approximately equal to the total activity recovered in an anti-GFP immunoprecipitate. The endogenous AMPK-α2 activity in CCL13 cells was much lower than the endogenous α1 activity and was barely detectable. This is consistent with our findings that endogenous α1, but not α2, was detectable by Western blotting in CCL13 cell lysates (see above). As expected, anti-α2 antibody did not precipitate any additional activity on expression of either α1 or GFP–α1. For reasons that remain unclear, the activities of recombinant α2 or GFP–α2 complexes expressed in CCL13 cells were low and difficult to measure accurately. However, we could clearly demonstrate that both the α2 and the GFP–α2 complexes were active when expressed in Chinese hamster ovary cells (Table 4). As in CCL13 cells, the activity of endogenous α2 complexes was negligible, whereas that of endogenous α1 complexes was clearly measurable (20–40 pmol/min per mg). A significant increase in activity precipitable with anti-α2 antibody was obtained on expression of recombinant α2 or GFP–α2. A small but detectable increase in activity precipitable with anti-GFP antibody was also observed on expression of recombinant GFP–α2, but not of α2.

Confocal microscopy of the transfected INS-1 cells showed that co-expression of GFP–α1 and γ1, with either β1 or β2, resulted in a diffuse cytoplasmic fluorescence with only very weak fluorescence in the nucleus (Figures 7A and 7B). The ratio of cytoplasmic to nuclear mean pixel intensity was 8.7 ± 3.3 (10) for $\alpha1\beta1\gamma1$ and 7.7 ± 2.1 (8) for $\alpha1\beta2\gamma1$ (means $\pm$ S.E.M., with numbers of cells in parentheses). In contrast, co-expression of GFP–α2 and γ1 with either β1 or β2 resulted in a different pattern that was consistent with the results from the use of indirect immunofluorescence in paraformaldehyde-fixed cells (Figures 7C and 7D). There was strong cytoplasmic fluorescence but there was also significant nuclear fluorescence that was excluded from the nucleoli. In this case the ratio of cytoplasmic to nuclear intensity was 2.8 ± 0.9 (10) for $\alpha2\beta1\gamma1$ and 2.8 ± 0.5 (14) for $\alpha2\beta2\gamma1$. The cytoplasmic-to-nuclear ratios were significantly different ($P < 0.02$) when the expressions of GFP–α1 and GFP–α2 isoforms were compared, but were not significantly different when expressions of β1 and β2 were compared. Expression of GFP alone gave a pattern different from that with either GFP–α1 or GFP–α2, in which the fluorescence was evenly distributed throughout the cell (Figures 7E and 7F).

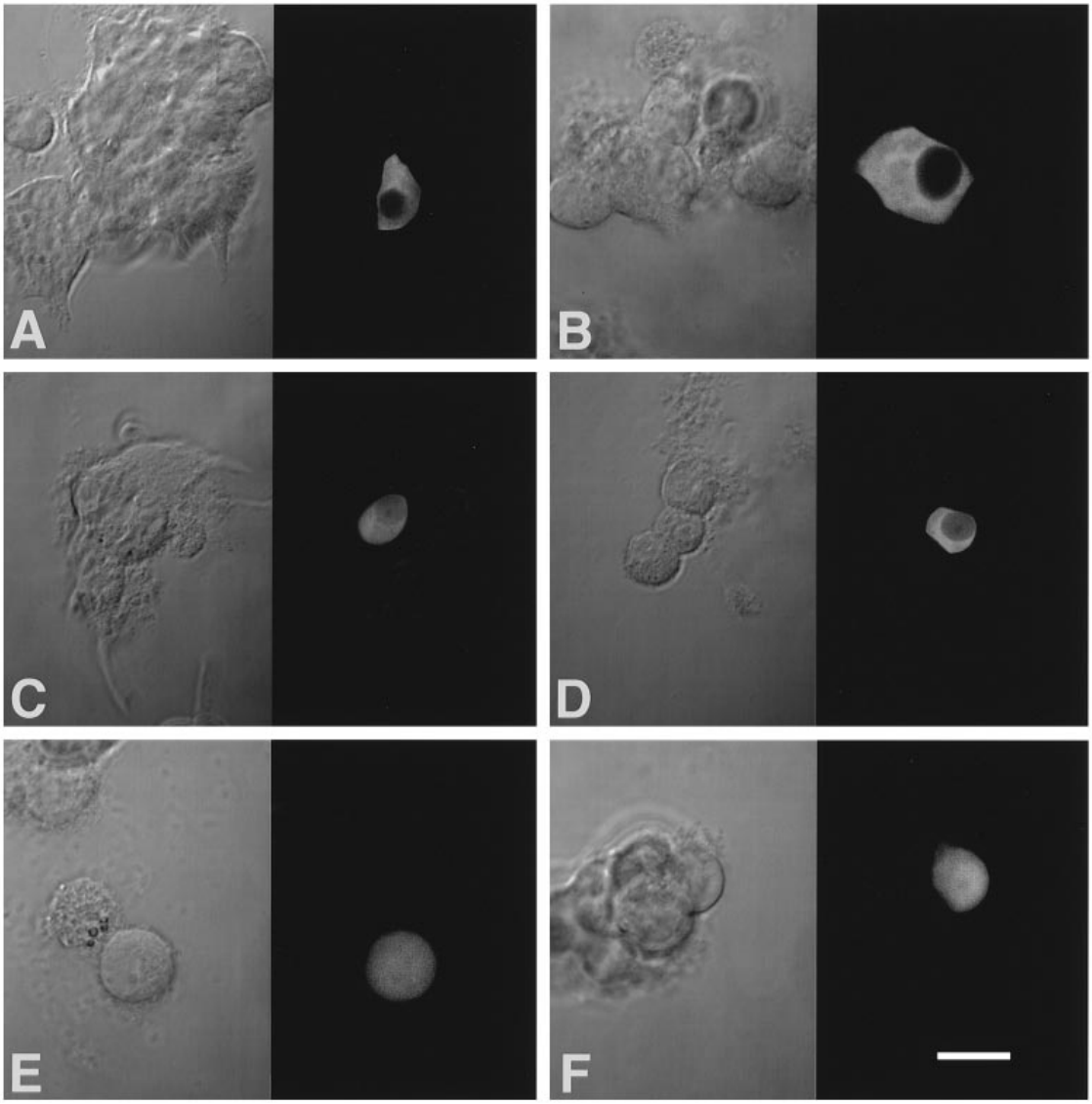

Figure 7 Live INS-1 cells after co-transfection with plasmids encoding GFP–α1, β1 and γ1 (A), GFP–α1, β2 and γ1 (B), GFP–α2, β1 and γ1 (C), GFP–α2, β2 and γ1 (D), GFP, β1 and γ1 (E), or GFP, β2 and γ1 (F)

Cells were observed by bright-field illumination (left panel in each pair) or by confocal microscopy (right panel in each pair). Scale bar, 12.5 μm.

Table 3 AMPK activity in immunoprecipitates from lysates of CCL13 cells transfected with DNA species encoding free GFP, free α1 or a GFP–α1 fusion

Immunoprecipitates were prepared with anti-α1, anti-α2 or anti-GFP antibodies, resuspended, then assayed for AMPK activity. The results are expressed as means $\pm$ S.E.M. for three replicate assays.

	AMPK activity (pmol/min per mg of lysate protein)		
Antibody	GFP	α1	GFP–α1
Anti-α1	5.5 $\pm$ 1.4	11.1 $\pm$ 8.0	14.1 $\pm$ 4.9
Anti-α2	1.1 $\pm$ 0.5	0.5 $\pm$ 0.1	0.5 $\pm$ 0.3
Anti-GFP	0.09 $\pm$ 0.04	0.1 $\pm$ 0.2	4.5 $\pm$ 1.0

Table 4 AMPK activity in immunoprecipitates from lysates of Chinese hamster ovary cells transfected with DNA species encoding free GFP, free α2 or a GFP–α2 fusion

Immunoprecipitates were prepared with anti-α1, anti-α2 or anti-GFP antibodies, resuspended, then assayed for AMPK activity. The results are expressed as means $\pm$ S.E.M. for three replicate assays. Abbreviation: n.s., activity not significantly different from the blank.

	AMPK activity (pmol/min per mg of lysate protein)		
Antibody	GFP	α2	GFP–α2
Anti-α1	22 $\pm$ 2	42 $\pm$ 6	42 $\pm$ 4
Anti-α2	0.39 $\pm$ 0.11	9.5 $\pm$ 0.9	2.2 $\pm$ 0.2
Anti-GFP	n.s.	0.21 $\pm$ 0.03	0.77 $\pm$ 0.28

Very similar results were obtained on the expression of GFP fusions in CCL13 cells (results not shown). In these cells, activation of AMPK by treatment with 500 μM arsenite did not affect the nuclear-to-cytoplasmic ratio.

DISCUSSION

This study has revealed at least three significant functional differences between AMPK complexes containing the α1 or α2 isoform of the catalytic subunit, as follows.

1. Although both are sensitive to 5′-AMP in the same low micromolar concentration range, the α2 complex was stimulated to a much larger extent (5–6-fold) than the α1 complex (less than 2-fold). Reactivation of the complex by an upstream kinase was also stimulated by AMP to a much greater extent for the α2 complex (5-fold) than the α1 complex (2-fold).

2. Although both α1 and α2 seem capable of being activated by the same upstream kinase, i.e. AMPKK or CaMKK, and were inactivated at similar rates by PP2C, the α1 isoform was more resistant than α2 to inactivation by PP2A.

3. By three independent methods, i.e. (i) blotting of nuclear fractions, (ii) indirect immunofluorescence of endogenous AMPK in fixed cells, and (iii) fluorescence of GFP fusions in intact, living cells, there was a clear and consistent difference in the subcellular localization of the α1 and α2 isoforms, with α2 being at least partly nuclear.

The lower degree of stimulation of α1 complexes by AMP was observed not only in α1- and α2-specific preparations made by immunodepletion of the purified kinase, but also in immunoprecipitates made after steps 1 and 2 of the purification procedure, showing that it was not an artifact caused by selective loss of AMP-dependence during purification. Preparations containing both α1 and α2 isoforms, made either by conventional purification or by immunoprecipitation with an anti-γ antibody that precipitates all of the kinase activity, have an intermediate degree of AMP stimulation (3–4-fold). We have previously discussed a model for the allosteric effects of AMP, with a version of the Monod–Wyman–Changeux model for allosteric enzymes [38], in which AMPK exists in an equilibrium between a less active 'T' conformation and a more active 'R' conformation, the latter being stabilized by the binding of AMP [1]. The results in the present paper can be explained on the basis of this model by assuming that, in the absence of AMP, α1 complexes exist as approx. 1:1 mixtures of R and T forms, whereas for α2 complexes the equilibrium ratio (R to T) is approx. 1:4.

In the dephosphorylation experiments (Figure 2) the α1 complex was probably present at a slightly lower molar concentration than the α2 complex. Nevertheless with the same concentrations of phosphatase the two isoforms were inactivated by Mg^{2+} and PP2C at comparable rates but the α2 complex was dephosphorylated by PP2A much more readily than the α1 complex (Figure 2). We have previously shown that the primary site phosphorylated by AMPKK on AMPK is Thr-172 [32]. Although it was not realized at the time, these experiments were performed with a preparation that was a mixture of α2 and α1 complexes. The sequence in the immediate vicinity of Thr-172 is identical between α1 and α2, and it might have been expected that Thr-172 would be dephosphorylated at similar rates in both isoforms. However, recent site-directed mutagenesis studies (A. Woods and D. Carling, unpublished work) have suggested that sites additional to Thr-172 might also be required for activation by AMPKK and that these might differ in their susceptibility to dephosphorylation.

The results in Figure 2 also show that AMPKK reactivates the α1 and α2 complexes with equal facility. This preparation of AMPKK was purified 300-fold from rat liver; the assay used was its ability to reactivate rat liver AMPK [32]. We now know [16] that the latter is a mixture of the α2 and α1 isoforms. There was no evidence during the purification of AMPKK [32] for the separation of other AMPK-reactivating activities. Although the AMPKK preparation is not homogeneous and we cannot rule out the possibility that it contains distinct α1- and α2-reactivating kinases, we consider this to be unlikely. Figure 3 shows that the α1 and α2 complexes are reactivated at similar rates by homogeneous CaMKK. Although the activation of AMPK by CaMKK might not have any physiological relevance, this result does show that the same upstream kinase can reactivate both complexes *in vitro* and argues against the possibility that there are distinct, specific upstream kinases for α1 and α2 complexes *in vivo*.

The regulation of AMPK by AMP, and by phosphorylation, could conceivably have been affected by the isoforms of the β and γ subunits that were present. However, the predominant forms in rat liver are β1 [accounting for more than 95% of total AMPK activity (C. Thornton, M. A. Snowden and D. Carling, unpublished work)] and γ1 [more than 90% of total AMPK activity (P. C. F. Cheung and D. Carling, unpublished work)]. Moreover, the β1 and β2 isoforms readily form complexes with either α1 or α2 [19]. Finally, the available evidence indicates that both AMP binding [39] and the regulation of activity by phosphorylation [32] are functions of the catalytic α subunits. The differences obtained between α1 and α2 complexes in Figures 1–3 are therefore unlikely to have been due to association with different β or γ subunits.

Perhaps the most interesting conclusions of the present study were the findings that the α1 and α2 complexes have different subcellular localizations. Both were present in the cytoplasm of INS-1 cells and CCL13 cells, but α2 was clearly also localized in the nuclei of both cell types with all approaches utilized (Western blotting of nuclear preparations in INS-1 cells, indirect immunofluorescence and expression of GFP fusions in both cell types). We did not obtain any evidence for a relocalization of AMPK between the cytoplasm and nucleus when the kinase was activated, either by glucose starvation (which activates the kinase in INS-1 cells) or with arsenite treatment of CCL13 cells expressing the GFP fusions. The indirect immunofluorescence and the GFP fusion approaches both indicated that α2 complexes are spread diffusely throughout the nucleus, although they are excluded from nucleoli. Although each of the three approaches utilized have potential pitfalls, a qualitatively similar result was obtained with each of these complementary methods. This makes it very unlikely that the apparent nuclear localization was an artifact of one of the techniques utilized, e.g. (1) that the anti-α2 antibodies cross-react non-specifically with another nuclear protein, (2) that the GFP fusion causes misdirection of the protein to an inappropriate location, or (3) that the GFP–α2 fusion is degraded to release free GFP. The latter possibility was also ruled out by the results of Western blotting with anti-GFP antibodies (Figure 6). Western blotting of nuclear proteins (Figure 4) indicated that α2 complexes are highly enriched in the nuclei of INS-1 cells. The nuclear enrichment was less marked with the immunofluorescence and GFP fusion methods (Figures 5 and 7). It should be noted that none of these methods is likely to give accurate quantification of the distribution, although the blotting approach is perhaps the most quantitative.

Western blotting of CCL13 cell lysates (Figure 6) showed that the GFP–α subunit fusions are expressed at similar levels to those of transfected free α subunits, and confirms that the proteolytic degradation of the fusion proteins within the cells was negligible. Expression of the recombinant proteins in CCL13

or Chinese hamster ovary cells followed by immunoprecipitation show that the GFP–α1 (Table 3) and GFP–α2 (Table 4) fusions are active, suggesting that the kinase can fold into its native state despite the presence of the 27 kDa GFP fused at the N-terminus of the α subunit.

One thing that remains unclear is the mechanism by which the α2 complexes are directed to the nucleus. The heterotrimeric AMPK complex has a molecular mass of approx. 200 kDa [11], making it very unlikely that it could diffuse through nuclear pores without an active transport mechanism. None of the known AMPK subunits has a classical nuclear localization signal, so the α2 complexes either contain a novel nuclear localization signal or they are directed to the nucleus by association with some other targeting protein. The targeting does not seem to be a function of the β subunits because GFP–α2 was directed to the nucleus, whereas GFP–α1 was excluded, when they were co-expressed with either β1 or β2. Our findings that recombinant GFP–α1 and GFP–α2 fusions are targeted to the correct subcellular locations introduces the possibility of studying the targeting mechanism by site-directed mutagenesis.

The indirect immunofluorescence approach (Figure 5) also gave indications that there were subtle differences in subcytoplasmic localization between α1 and α2 complexes. The α2 complexes seemed to give a punctate distribution, whereas the α1 complexes were more diffuse, with some indications of association with the plasma membrane. The punctate distribution of cytoplasmic α2 complexes was not evident in the results for the GFP fusions in Figure 7. However, under different incubation conditions we have seen a punctate distribution of cytoplasmic GFP–α2 in CCL13 (results not shown), and this is the subject of continuing investigations. Identification of the subcellular structures involved will require co-localization studies, or the increased resolution of the electron microscope.

The β1 subunit of AMPK is myristoylated at the N-terminus [40], and the β2 subunit also contains a potential myristoylation sequence [19]. Mitchelhill et al. [40] found that wild-type AMPK complexes expressed in COS-7 cells were recovered in 150000 ***g*** pellets, whereas complexes containing non-myristoylated mutants of β1 were partly recovered in the soluble fraction. However, it seems unlikely that myristoylation of the β subunit could be involved in targeting to specific subcellular locations.

Although in previous work we reported that there was a small difference between α1 and α2 in terms of the requirement for a hydrophobic side chain at the P+4 position in peptide substrates [16], this was not confirmed by the more detailed studies reported here. Replacement of the leucine at the P+4 position in the peptide AMARAASAAALARRR with glycine resulted in more than 100-fold increases in K_m in both cases. The reason for the discrepancy with our previous work is not clear, although the standard errors in the measurements made with α2 at a single concentration of AMARAASAAAGARRR [16] were rather large. We were interested in the effect of the P+4 position because Michell et al. [41] reported, after using the α1 complex purified from rat liver on a peptide affinity column, that a hydrophobic residue at this position was not necessary. Our present results are not in agreement with this. The basis for the conclusion by Michell et al. was that the peptide LKKLTRR-PSFSAQ (the first serine residue being phosphorylated), which has a glutamine residue at the P+4 position, was a good substrate with a K_m of 4 μM. There would seem to be at least two ways of resolving this apparent discrepancy: (1) the side chain of glutamine, although not hydrophobic, is bulky and uncharged, and it is possible that it can be accommodated in the putative hydrophobic pocket that binds the P+4 residue; (2) it is possible that a hydrophobic residue at the P+4 position is preferred, but not essential if there are a sufficient number of other positive determinants. Other subtle differences in peptide specificity were reported in our original comparison of α1 and α2: for example, the α1 form had a stronger preference for the basic residue being at P−3 rather than P−4 [16]. However, we now suspect that the specificity of the different isoforms of AMPK for downstream targets might result more from different subcellular localizations than from different intrinsic specificities.

The findings in the present paper that α1 and α2 complexes have different dependences on AMP, coupled with the findings that they are targeted to different subcellular locations, raises the interesting possibility that responses to ATP depletion could be different in distinct cell types and subcellular locations. This might explain, for example, why activation of AMPK by electrical stimulation of isolated muscle was apparently confined to the α2 isoform [20]. The nuclear localization of α2 complexes also raises the intriguing possibility that AMPK might regulate gene expression in response to cellular stresses associated with ATP depletion. The yeast homologue of the AMPK α subunit, Snf1p, is reported to be present in both the cytoplasm and the nucleus of *S. cerevisiae* [29], as is the γ subunit homologue, Snf4p [21]. Genetic evidence [42,43] shows that the yeast SNF1 complex is involved in regulating gene expression. A likely target of the SNF1 complex *in vivo* is the transcription factor Mig1p, whose ability to repress transcription from glucose-repressed genes is relieved by SNF1 activation, probably via direct phosphorylation [44–46]. Our results now suggest that the AMPK-α2 complex could also act, at least in part, by the phosphorylation of transcription factors, a possibility that we are actively pursuing.

We thank Steve Davies for purified AMPK, Angus Lamond and Judith Sleeman for anti-coilin antibodies and the plasmid phGFPmcs, Nick Helps for PP2C, Art Edelman (Buffalo) for CaMKK, and Guy Rutter (Bristol) for INS-1 cells. This study was supported by a Programme Grant from the Wellcome Trust (D.G.H.), Unit support from the Medical Research Council (D.C.), an Intermediate Fellowship from the British Heart Foundation (A.W.), and a BBSRC research studentship (I.S.).

REFERENCES

1 Hardie, D. G. and Carling, D. (1997) Eur. J. Biochem. **246**, 259–273
2 Corton, J. M., Gillespie, J. G. and Hardie, D. G. (1994) Curr. Biol. **4**, 315–324
3 Winder, W. W. and Hardie, D. G. (1996) Am. J. Physiol. **270**, E299–E304
4 Hutber, C. A., Hardie, D. G. and Winder, W. W. (1997) Am. J. Physiol. **272**, E262–E266
5 Kudo, N., Barr, A. J., Barr, R. L., Desai, S. and Lopaschuk, G. D. (1995) J. Biol. Chem. **270**, 17513–17520
6 Witters, L. A., Nordlund, A. C. and Marshall, L. (1991) Biochem. Biophys. Res. Commun. **181**, 1486–1492
7 Davies, S. P., Helps, N. R., Cohen, P. T. W. and Hardie, D. G. (1995) FEBS Lett. **377**, 421–425
8 Hawley, S. A., Selbert, M. A., Goldstein, E. G., Edelman, A. M., Carling, D. and Hardie, D. G. (1995) J. Biol. Chem. **270**, 27186–27191
9 Corton, J. M., Gillespie, J. G., Hawley, S. A. and Hardie, D. G. (1995) Eur. J. Biochem. **229**, 558–565
10 Merrill, G. M., Kurth, E., Hardie, D. G. and Winder, W. W. (1997) Am. J. Physiol. **36**, E1107–E1112
11 Davies, S. P., Hawley, S. A., Woods, A., Carling, D., Haystead, T. A. J. and Hardie, D. G. (1994) Eur. J. Biochem. **223**, 351–357
12 Gao, G., Fernandez, S., Stapleton, D., Auster, A. S., Widmer, J., Dyck, J. R. B., Kemp, B. E. and Witters, L. A. (1996) J. Biol. Chem. **271**, 8675–8681
13 Woods, A., Cheung, P. C. F., Smith, F. C., Davison, M. D., Scott, J., Beri, R. K. and Carling, D. (1996) J. Biol. Chem. **271**, 10282–10290
14 Carling, D., Aguan, K., Woods, A., Verhoeven, A. J. M., Beri, R. K., Brennan, C. H., Sidebottom, C., Davison, M. D. and Scott, J. (1994) J. Biol. Chem. **269**, 11442–11448
15 Dyck, J. R. B., Gao, G., Widmer, J., Stapleton, D., Fernandez, C. S., Kemp, B. E. and Witters, L. A. (1996) J. Biol. Chem. **271**, 17798–17803
16 Woods, A., Salt, I., Scott, J., Hardie, D. G. and Carling, D. (1996) FEBS Lett. **397**, 347–351

17 Stapleton, D., Mitchelhill, K. I., Gao, G., Widmer, J., Michell, B. J., Teh, T., House, C. M., Fernandez, C. S., Cox, T., Witters, L. A. and Kemp, B. E. (1996) J. Biol. Chem. **271**, 611–614
18 Stapleton, D., Woollatt, E., Mitchelhill, K. I., Nicholl, J. K., Fernandez, C. S., Michell, B. J., Witters, L. A., Power, D. A., Sutherland, G. R. and Kemp, B. E. (1997) FEBS Lett. **409**, 452–456
19 Thornton, C., Snowden, M. A. and Carling, D. (1998) J. Biol. Chem. **273**, 12443–12450
20 Vavvas, D., Apazidis, A., Saha, A. K., Gamble, J., Patel, A., Kemp, B. E., Witters, L. A. and Ruderman, N. B. (1997) J. Biol. Chem. **272**, 13255–13261
21 Celenza, J. L., Eng, F. J. and Carlson, M. (1989) Mol. Cell. Biol. **9**, 5045–5054
22 Mitchelhill, K. I., Stapleton, D., Gao, G., House, C., Michell, B., Katsis, F., Witters, L. A. and Kemp, B. E. (1994) J. Biol. Chem. **269**, 2361–2364
23 Wilson, W. A., Hawley, S. A. and Hardie, D. G. (1996) Curr. Biol. **6**, 1426–1434
24 Yang, X., Jiang, R. and Carlson, M. (1994) EMBO J. **13**, 5878–5886
25 Jiang, R. and Carlson, M. (1997) Mol. Cell. Biol. **17**, 2099–2106
26 Davies, S. P., Carling, D., Munday, M. R. and Hardie, D. G. (1992) Eur. J. Biochem. **203**, 615–623
27 Witters, L. A. and Watts, T. D. (1990) Biochem. Biophys. Res. Commun. **169**, 369–376
28 Woods, A., Munday, M. R., Scott, J., Yang, X., Carlson, M. and Carling, D. (1994) J. Biol. Chem. **269**, 19509–19515
29 Celenza, J. L. and Carlson, M. (1986) Science **233**, 1175–1180
30 Carlson, M., Osmond, B. C. and Botstein, D. (1981) Genetics **98**, 25–40
31 Neigeborn, L. and Carlson, M. (1984) Genetics **108**, 845–858
32 Hawley, S. A., Davison, M., Woods, A., Davies, S. P., Beri, R. K., Carling, D. and Hardie, D. G. (1996) J. Biol. Chem. **271**, 27879–27887
33 Cohen, P., Alemany, S., Hemmings, B. A., Resink, T. J., Strålfors, P. and Lim, T. H. (1988) Methods Enzymol. **159**, 390–408
34 Edelman, A. M., Mitchelhill, K. I., Selbert, M. A., Anderson, K. A., Hook, S. S., Stapleton, D., Goldstein, E. G., Means, A. R. and Kemp, B. E. (1996) J. Biol. Chem. **271**, 10806–10810
35 Davies, S. P., Carling, D. and Hardie, D. G. (1989) Eur. J. Biochem. **186**, 123–128
36 Dale, S., Wilson, W. A., Edelman, A. M. and Hardie, D. G. (1995) FEBS Lett. **361**, 191–195
37 McGowan, C. H. and Cohen, P. (1988) Methods Enzymol. **159**, 416–426
38 Monod, J., Wyman, J. and Changeux, J. P. (1965) J. Mol. Biol. **12**, 88–118
39 Carling, D., Clarke, P. R., Zammit, V. A. and Hardie, D. G. (1989) Eur. J. Biochem. **186**, 129–136
40 Mitchelhill, K. I., Michell, B. J., House, C. M., Stapleton, D., Dyck, J., Gamble, J., Ullrich, C., Witters, L. A. and Kemp, B. E. (1997) J. Biol. Chem. **272**, 24475–24479
41 Michell, B. J., Stapleton, D., Mitchelhill, K. I., House, C. M., Katsis, F., Witters, L. A. and Kemp, B. E. (1996) J. Biol. Chem. **271**, 28445–28450
42 Gancedo, J. M. (1992) Eur. J. Biochem. **206**, 297–313
43 Ronne, H. (1995) Trends Genet. **11**, 12–17
44 Treitel, M. A. and Carlson, M. (1995) Proc. Natl. Acad. Sci. U.S.A. **92**, 3132–3136
45 Ostling, J., Carlberg, M. and Ronne, H. (1996) Mol. Cell. Biol. **16**, 753–761
46 Ostling, J. and Ronne, H. (1998) Eur. J. Biochem. **252**, 162–168

Received 20 March 1998/14 May 1998; accepted 27 May 1998